Macromolecules **2004,** *37,* 7742−7746

Structure of Polystyrene at the Interface with Various Liquids

Clayton S.-C. Yang, Philip T. Wilson,[†] and Lee J. Richter*

National Institute of Standards and Technology, 100 Bureau Drive,
Gaithersburg, Maryland 20899-8372

Received February 13, 2004; Revised Manuscript Received June 21, 2004

ABSTRACT: Vibrationally resonant sum frequency generation (VR-SFG) is used to determine the structure of the phenyl side groups of deuterated polystyrene at the liquid/solid interface for the nonsolvent liquids hexane, methanol, ethanol, glycerol, and water. The structure for the three low-surface-tension (γ) liquids—hexane, methanol, and ethanol—is similar and only slightly perturbed from that of the air/solid interface. The air interface is ordered with the phenyl rings oriented away from the polymer bulk. The structure for the two high-γ liquids, water and glycerol, differs significantly from the low-γ liquids and reflects a near flat orientation of the phenyl ring.

Introduction

Polymer interfaces, both solid/solid and solid/liquid, are critical to a diverse array of technologies, ranging from adhesives through corrosion-resistant coatings and lubricating films to biosensors and medical implants. The molecular structure of these interfaces has proven difficult to characterize as traditional surface-sensitive diagnostics lack the necessary in-situ performance or interface selectivity. Vibrationally resonant sum-frequency-generation (VR-SFG) has emerged as a powerful tool for the in-situ study of interfaces[1−5] and has recently been applied with success to the study of polymer systems.[6] As a second-order nonlinear optical process, VR-SFG has inherent interface specificity. Signals from centrosymmetric bulk media, such as all liquids, are forbidden in the dipole approximation. Additionally, VR-SFG has the advantage, with respect to linear optical techniques, that it can determine both the alignment and orientation of functional groups at an interface.

Polystyrene (PS) is a simple vinyl polymer and serves as a model system for diverse studies of polymer physics. Recently, VR-SFG has been used to characterize the structure[7−9] and dynamics[10] of the air/PS interface and the structure of buried PS/solid interfaces.[11−13] In our study of buried PS interfaces,[13] we found that the orientation distribution of the phenyl side groups varied significantly between low surface energy, hydrophobic substrates and high surface energy, hydrophilic substrates. On hydrophobic substrates, the phenyl side group structure was similar to that found at the air/PS interface, with the phenyl group oriented away from the polymer bulk. On the hydrophilic substrates, the phenyl group adopted a more lying flat orientation and twisted with respect to the chain backbone. This twisted configuration was attributed to the development of a π-hydrogen bond between the phenyl ring and surface hydroxy groups. The increased polymer substrate interaction was reflected in improved adhesion between the film and the substrate. The PS structure on the hydrophilic substrate was similar to that reported for sapphire substrates.[11] In the present paper, we present in-situ VR-SFG studies of the interface of deuterated polystyrene (dPS) with a variety of liquids (hexane, methanol, ethanol, glycerol, and water) to further explore the relationship between interfacial energy and PS interface structure.

Experiment

The experiments were performed with a broad-bandwidth VR-SFG apparatus that has been described previously.[14] In brief, broadband (>150 cm^{-1} fwhm) IR pulses, derived from an ≈110 fs, 1 kHz, regeneratively amplified Ti-sapphire laser system, were temporally and spatially overlapped with narrow-bandwidth (≈3 cm^{-1}) 794 nm VIS pulses at the sample. The resolution of the VR-SFG spectra was limited by the bandwidth of this visible probe. The SUM light at about 672 nm was collected and dispersed with a spectrometer. A scientific grade CCD detector was used to detect the entire SUM spectrum in parallel. Experiments reported herein used broad-bandwidth IR pulses in the wavenumber range of 1900−2300 cm^{-1}. Pairs of half-wave plates and polarizers were used to control the polarization of the IR, VIS, and SUM beams. The polarizers are placed between the sample and wave plate to eliminate any nonidealities in the achromatic wave plates. All VR-SFG spectra reported were taken with either SSP (SUM: S, VIS: S, IR: P) or SPS (SUM: S, VIS: P, IR: S) polarization combinations. S polarization is defined as having an electric vector perpendicular to both the incident wavevector k and the outward surface normal n, while the electric vector for P polarization is defined as $S \times k$ and lies in the plane of incidence. All spectra are referenced to the spectrum of an octadecanethiol (ODT) self-assembled monolayer on Au. The ODT film has no vibrational features in the 1900−2300 cm^{-1} range. For ease of comparison with linear vibrational spectroscopies, the x-axis is set to the incident IR wavenumber.

The thin polymer films (≈332 nm) were formed by spin-coating 220 000 number-average relative molecular mass, narrow-distribution ($M_w/M_n = 1.04$) atactic dPS from Polymer Source Inc.,[15] at 2000 rpm from toluene solutions onto Au films (≈200 nm thick) evaporated onto microaqueduct slides (see below). The polymer films were annealed under vacuum for 2 h at 120 °C. The Au films were cleaned prior to polymer spin-coating by 15 min UV-ozone treatment, followed by rinsing with ethanol to reduce the resultant thin Au oxide layer and then toluene. The Au surfaces were hydrophilic (water contact angle less than 3°) and showed negligible VR-SFG signatures in the CD and CH regions. The thicknesses of the dPS films were determined by spectroscopic ellipsometry and are accurate to ≈1 nm. All dPS films were rinsed with ethanol and dried with N_2 prior to assembly in the in-situ cell. Previous studies of the PS/air interface[8] established that, even with the

---

[†] Current address: Milliken Research Corporation, 920 Milliken Road, Spartanburg, SC 29303.

[*] Corresponding author: e-mail lee.richter@nist.gov.

10.1021/ma049692s

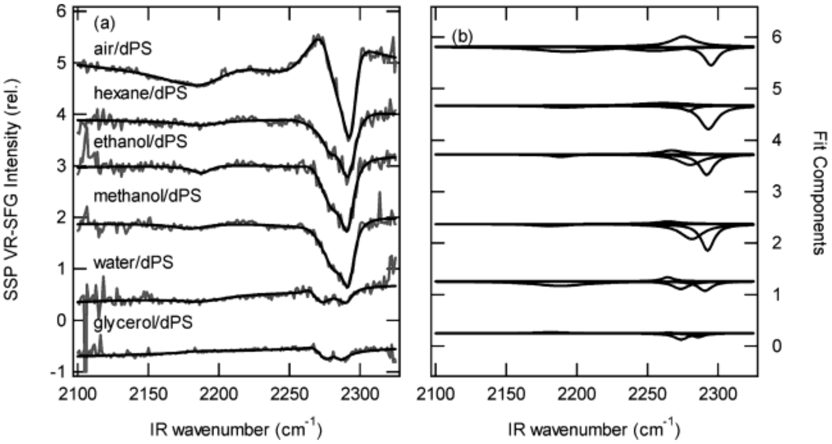

Figure 1. (a) SSP VR-SFG spectra from the dPS films while in air and in contact with the five liquids hexane, methanol, ethanol, water, and glycerol. The smooth solid lines shown are fits of the spectra to eq 1. (b). The imaginary part of the individual Lorentzian components of the fits.

precaution of using an oil-free diaphragm pumped oven, adventitious hydrocarbon is typically found on the surface of freshly prepared films. This could be removed by an ethanol rinse, with no apparent degradation to the polymer/air interface.

The sample cell was a model FCS2 microscopy chamber from Bioptechs (Butler, PA).[15] Technical details are available online.[16] A 25 μm Teflon spacer was sandwiched between a 1 mm calcium fluoride entrance window and a polymer-gold-coated microaqueduct slide inside the chamber. The microaqueduct slide is engineered to provide laminar flow in an $\approx$12 mm wide by 20 mm long channel across the sample. The nominal volume of the flow cell was 6 μL. A peristaltic pump was used to push solution through the cell at a flow rate of about 1.1 mL/min. A series of five, 2 min long VR-SFG spectra were acquired, beginning upon the complete wetting of the film. The surface was kept in contact with flowing liquid throughout the collection of VR-SFG spectra. A 25 mL glass jar was used as a sample reservoir, and stainless steel tubing ($\approx$0.6 mm i.d.) connected the reservoir and the pump to the sample cell. The IR and visible beams were coincident on the calcium fluoride window at 74° and 55°. Because of refraction, the incident angles were nominally 45° and 37° at the solution/Au interface. The organic liquids were spectroscopy grade and used as received. The water was obtained from a Barnstead Nanopure system[15] with a final resistivity >18 MΩ cm.

The IR and Raman reference spectra were acquired with a Nicolet Magna-IR 860 FTIR at 2 cm^{-1} resolution and a Bruker RFS100 FT-Raman (1064 nm excitation) at 2 cm^{-1} resolution, respectively. FTIR spectra were recorded in reflection from a $\sim$100 nm thick film. FT-Raman spectra were recorded in 180° configuration from the powder. Reported frequencies are from multiple Lorentzian fits to the spectra.

Results

Shown in Figure 1a are SSP VR-SFG spectra from the dPS films while in air and in contact with the five liquids. We report the average of the five 2 min spectra. The resonant features between 2100 and 2300 cm^{-1} can be attributed to the C$-$D stretching vibrational modes of the dPS (see below). In general, there are three possible origins of the VR-SFG signal: the top (ambient/polymer) interface, the bulk of the polymer, or the buried (polymer/Au) interface. Previous studies of PS films have determined that bulk mixing is negligible.[8] For thin films on reflective substrates, the relative sensitivity to the top and buried interfaces is a function of film thickness due to the standing waves created by the incident and outgoing fields. We have demonstrated that this can be used to isolate the contributions from each interface.[12] The thickness of the dPS used in this experiment (332 nm) was chosen to isolate the contribution to the VR-SFG signal from the ambient/polymer interfaces. This was verified by observing the elimination of vibrational features in the VR-SFG signal after films were treated with UV-ozone exposure which has been shown to severely disturb the order of the phenyl pendant rings at the polymer surface.[7,13] Details of the dPS thickness dependence of the expected signal and the UV-ozone exposure tests are provided as Supporting Information.

The VR-SFG spectrum from an isotropic interface in SSP and SPS configurations can be modeled by the form

$$I_{\mathrm{ssp,sps}} = \frac{1}{|\chi^{\mathrm{e}}_{\mathrm{ssp,sps}}|^2}\left| B\mathrm{e}^{i\phi} + \sum_i \frac{A_i}{\nu_{\mathrm{IR}} - \nu_i + i\,\Gamma_i}\right|^2 \quad (1)$$

where B corresponds to the nonresonant signal and the sum is over the vibrationally resonant contributions from the adsorbate molecules.[17] The factor ϕ is the phase difference between the features of the spectra and the nonresonant background. A, ν, and Γ correspond to the amplitude, resonant wavenumber, and line width of each resonant feature, respectively. χ^{e} is the effective nonlinear susceptibility of the reference sample. Solid lines shown in Figure 1a are fits of the spectra to this form, with four resonant features between 2100 and 2300 cm^{-1}. The imaginary part of the individual resonant terms, $A_i\Gamma_i/[(\nu_{\mathrm{IR}} - \nu_i)^2 + \Gamma_i^2]$, is shown in Figure 1b. The feature near 2190 cm^{-1} is attributed to the CD$_2$ asymmetric stretch of the polymer backbone. The high-wavenumber features can be attributed to CD stretches of the pendant rings on the basis of IR and Raman spectra, as shown in Table 1. The mode assignments are based on literature assignments for similar substituted benzenes[18] and comparison to density functional theory calculations[19,20] for the model compound isopropylbenzene and employ Wilson notation for the normal modes of benzene.[18]

The VR-SFG spectra of dPS at the low surface tension (γ) liquid interfaces (γ = 18.4 mN/m hexane, 22.6 mN/m methanol, 22.7 mN/m ethanol)[21] are qualitatively similar to that of dPS in air. The ν_2 aromatic CD stretching mode near 2292 cm^{-1} is the dominant feature. However, the spectra of dPS films in contact with high γ (72.8 mN/m water, 63.4 mN/m glycerol)[21] liquids are very different; most notably, the intensity of all features decreases significantly. For all five liquids, the spectral

Table 1. Vibrational Mode Assignments of Observed VR-SFG Features (in cm^{-1})

assignment	VR-SFG air	VR-SFG hexane	VR-SFG ethanol	VR-SFG methanol	VR-SFG water	VR-SFG glycerol	Raman	IR	DFT[a]
2	2295	2292	2292	2293	2289	2286	2286	2286	2286
20B	unres	2278	2280	2281	2275	2275		2272	2273
13	2275	2262	2267	2264	2261	2266	2264		2263
7B							2255		2251
7A							2234	2236	2247
CD_2 asym	2191	2186	2189	2181	2189	2182	2195	2195	

[a] Theoretical wavenumbers have been scaled by 0.962 to give agreement for ν_2.

change occurred within the measurement time (2 min) upon introduction of the liquid. No additional spectral changes were observed over the 10 min total elapsed time of the measurement. For all five liquids, a hexane-like spectrum was recorded upon removal of the liquid from the cell. The air spectrum was recovered after ethanol rinsing of the surface. This may be attributed to the presence of a hydrophobic contamination layer, deposited as the air/liquid interface traversed the film. This is consistent with a ~1 nm thickness increase observed with spectroscopic ellipsometry that was removed by the ethanol rinse. The radical differences between the water and glycerol interface spectra and the low-γ liquid interface spectra indicate that the contamination is not significant at the fully wet interface. Similarly, as an ethanol rinse regenerated the air/polymer interface, it is unlikely that the contamination influences the low-γ liquid interface spectra. An alternate explanation for the irreversibility of the air interface spectrum is liquid-induced morphology changes in the surface structure, which are then "solvent annealed" by the ethanol rinse. Surface restructuring has been observed by AFM for low molecular weight PS in water.[22]

The wavenumber of the dominant ν_2 feature is sensitive to environment, shifting from 2295 cm^{-1} for the air interface to 2289 cm^{-1} for the water interface. Similar behavior has been observed for the ν_2 feature for PS at the air and buried solid interface.[12,13] The resonant feature causing an increase in signal (due to constructive interference with the nonresonant background) at 2275 cm^{-1} for the air interface can be assigned to ν_{13} on the basis of the predicted relative phases of modes 13 and 2, as has been done for modes 7a and 2 for PS.[8,11] The resonant feature causing a signal decrease (due to destructive interference with the nonresonant background) at 2275 cm^{-1} for the water interface is attributed to ν_{20B}, with ν_{13} appearing as a weak constructive interference shoulder at 2261 cm^{-1}. The 20B mode cannot be resolved in the air interface spectrum. The extreme width of the CD_2 feature precludes meaningful analysis of its position. In general terms, the wavenumbers of the identified features at the air interface are perturbed from the bulk material, those at the water interface are more bulklike, and those at the hexane interface are intermediate.

The vector orientation of the observed functional groups (phenyl CD and backbone CD_2) can be determined by the sign of the phase ϕ between the vibrational resonance and the nonresonant background (B). It has been previously established that the phenyl rings are oriented away from the bulk of the polymer at the air interface.[8] The observation of similar destructive interference for ν_2 for all five liquids indicates that the phenyl rings are oriented into the liquid in all cases. It can be shown that the sign of the susceptibility for the B symmetry CD_2 asymmetric stretch is opposite to the A symmetry ν_2. Therefore, the observation of the CD_2 modes with destructive interference indicates that the CD_2 is oriented away from the liquid, consistent with simple connectivity arguments.

The orientation distribution of the phenyl rings of dPS at liquid/polymer interfaces can be quantitatively determined by the ratio of selected features in the SSP and SPS VR-SFG spectra of the interfaces. The details of this calculation have been described by many authors.[17,23,24] Following the notation of our earlier treatment of the PS/air interface,[8] it can be shown that

$$\frac{\langle\beta_i\rangle_{xzx}}{\langle\beta_i\rangle_{xxz}} = \frac{A_i^{\mathrm{sps}}F^{\mathrm{ssp}}}{A_i^{\mathrm{ssp}}F^{\mathrm{sps}}} \tag{2}$$

where β_i is the resonant molecular hyperpolarizability, A_i is the line amplitude from eq 1, and F is the combined Fresnel factor, accounting for the film thickness. $\langle\ \rangle$ denotes an average over the molecular orientation distribution defined in terms of the Euler angles: θ, tilt from the surface normal, and ψ, twist about the molecular axis. In general, SFG is only sensitive to low order moments of the orientation distribution; therefore, one must assume a trial distribution of a specific form. To determine both θ and ψ, one must observe at least two vibrational modes with different hyperpolarizability forms. Our spectra support quantitative analysis only for the strong feature due to ν_2; therefore, we have assumed a trial distribution function that is a delta function in θ and an isotropic average of ψ (equivalent to $\psi = 45°$). The analysis also requires knowledge of the hyperpolarizability tensor β_{ijk} for ν_2. We have assumed $\beta_{x'x'z'} = 0.86\beta_{z'z'z'}$ (prime indicates coordinates in the molecular frame), with all other elements 0, based on DFT calculations, and consistent with previous bond additive polarizability calculations: $\beta_{x'x'z'} \approx \beta_{z'z'z'}$.[25] Equation 2 then becomes

$$\frac{(r-2)\sin^2\theta}{r + r\cos^2\theta + 2\sin^2\theta} = \frac{A_i^{\mathrm{sps}}F^{\mathrm{ssp}}}{A_i^{\mathrm{ssp}}F^{\mathrm{sps}}} \tag{3}$$

where $r = \beta_{x'x'z'}/\beta_{z'z'z'}$.

SSP and SPS VR-SFG spectra of dPS films from the three characteristic interfaces—air/polymer, low-γ liquid (hexane)/polymer, and high-γ liquid (water)/polymer—are shown in Figure 2. The results from the fitting of model (1) are listed in Table 2 along with the Fresnel factors. In the calculation of the Fresnel factors, we have used the index of refraction for dPS and Au at the VIS and SUM frequencies obtained from spectroscopic ellipsometry.[26] The data in Table 2 combined with eq 3 enable us to determine the tilting angles of the interfacial phenyl ring group of dPS at the air/dPS interface (35 ± 4°), the hexane/dPS (42 ± 4°) interface, and the water/dPS (70 ± 8°) interface. The uncertainties are one

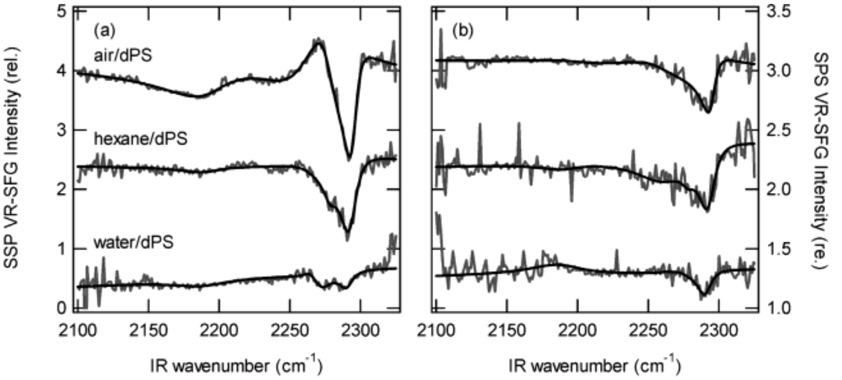

Figure 2. SSP (a) and SPS (b) VR-SFG spectra of dPS film from the three characteristic interfaces: air/polymer, low-γ liquid (hexane)/polymer, high-γ liquid (water)/polymer.

Table 2. VR-SFG Results for Various DPS Interfaces

interfaces	ν [cm^{-1}]	Γ_{ssp} [cm^{-1}]	A_{sps}/A_{ssp}	F_{ssp}/F_{sps}[a]	$\langle\beta\rangle_{xzx}/\langle\beta\rangle_{xxz}$
air/polymer	2295	5.8	0.12 ± 0.01	1.51	0.18 ± 0.02
hexane/polymer	2292	6.1	0.20 ± 0.02	1.16	0.23 ± 0.03
water/polymer	2289	6.1	0.32 ± 0.03	1.16	0.37 ± 0.05

[a] Calculated for $\lambda_{IR} = 4375$ nm, $\lambda_{VIS} = 794.5$ nm, $\lambda_{SUM} = 672.4$ nm, $n_{air} = 1$, $n_{hexane} = 1.378$, $n_{water} = 1.34$, $n_{dPS} = 1.53 + 0.011/\lambda^2$, $n_{Au}[\lambda_{IR}] = 3.03 + i\ 26.9$, $n_{Au}[\lambda_{VIS}] = 0.155 + i\ 4.71$, $n_{Au}[\lambda_{SUM}] = 0.178 + i\ 3.68$.

standard deviation and include the ≈10% precision in the A ratio, ≈10% precision in the Fresnel factor ratio (determined via propagation of the thickness uncertainties from the ellipsometric measurements), and an ≈10% estimated precision in the calculated r (determined via comparison of DFT and HF calculations[8] of r). The orientation of the phenyl rings at low-γ liquid/polymer interfaces is very similar to the one at the air/polymer interface, while that at high-γ liquid interfaces is clearly different. We must note in passing that the tilting angle of the interfacial phenyl ring group of dPS at the air/dPS interface reported here is smaller than the tilting angle of the interfacial phenyl ring group of PS at the air/PS interface (57 ± 8°) we reported in a previous study.[8] We do not believe this reflects an isotope effect in the interfacial orientation, but is due to uncharacterized systematic errors in the two analyses. The analysis of PS did not require assumption of a ψ distribution. Additionally, there are significant Fermi resonance interactions in the aromatic CH stretching region (the 20b mode of benzene is anharmonically resonant with three distinct combination bands[27]) that are not present in the CD region and that could introduce systematic errors in double harmonic approximation calculations of β.

Discussion

The possibility of surface reorganization in response to contact with a liquid has been recognized at least since Langmuir's original discussion of hydroxy groups on solid surfaces.[28] This reorganization has most commonly been characterized in the context of dynamic contact angle measurements,[21] although many other physical phenomena can contribute to a time-dependent contact angle. VR-SFG has been applied to the study of numerous liquid/polymer interfaces. The bulk of the studies have focused on the interaction of block copolymers[29] and polymer blends[30] with water and their subsequent reorganization, driven by the relative hydrophilicity of the components. The side group reorganization of the series of methacrylate polymers poly(methyl methacrylate) (PMMA), poly(butyl methacrylate) (PBMA), poly(octyl methacrylate) (POMA) has been characterized in water.[31,32] Significantly different behavior was observed for the three different alkyl chain lengths. Relatively little work has been done with liquids other than water.

In this study of dPS interfaces, there is a strong similarity between the air/polymer surface and the nonsolvent, low-γ liquid/polymer interfaces. This is consistent with previous PS/low-γ solid interface studies[13] and is consistent with the general concept that air is "hydrophobic". This is also consistent with the general similarity of the interface structure of albumin with air and various nonpolar liquids.[33,34] The PS/solid and PS/liquid interfaces differ in the flexibility of the nonpolymer component. The solid presumably acts as a rigid barrier, while the liquid can conform to maximize the interaction with the polymer. The conformational flexibility of the liquid seems to not significantly influence the polymer order, based on comparison of the three low-γ liquids studied here (hexane, methanol, ethanol) and the hydrophobic spin-on-glass previously characterized.[13] This is in marked contrast to the behavior of the low-γ (28.4 mN/m) solvent toluene. VR-SFG studies of the toluene vapor/PS interface have indicated complete randomization of the polymer surface, attributed to solvation of the phenyl groups.[35]

The interface of PS with the high surface tension, hydrogen-bonding liquids water and glycerol is very different from that of the low-γ liquids and air. In our previous study of the PS/hydroxylated spin-on-glass interface, it was found that the phenyl rings adopted a more tilted configuration, similar to the high tilt angle found here. In the case of the solid interface, there was strong evidence for a preferred twist of the phenyl ring with respect to the chain backbone, reflected in the atypically strong hyperpolarizability of the ν_{20B} feature. This twist was suggested to occur due to the development of a phenyl π-hydrogen bond interaction with the surface, and the constraint that the backbone must be in the plane of the surface. This strong ν_{20B} feature is not seen for the dPS/liquid interfaces. DFT calculations suggest that, unlike PS, the hyperpolarizability of ν_{20B}

for dPS does not become significantly perturbed when the ring is twisted with respect to the polymer backbone (see Supporting Information).

It is interesting to note that the alcohol interface is similar to the nonpolar hexane as opposed to the hydrogen-bonding water and glycerol. The dPS/alcohol data are consistent with the hypothesis that the alcohol orients at the hydrophobic polymer interface with the OH directed toward the liquid. Presumably this arises because the OH:O hydrogen-bonding interaction between the alcohol molecules is stronger than the weak OH:phenyl interaction. This is supported by VR-SFG studies of the alcohol/air interface, in which free OH features are not present, indicating that the OH is oriented into the liquid.[36]

Conclusions

We have characterized the side group order of polystyrene surfaces under various liquids. Combined with earlier work on polystyrene/solid interfaces, universal characteristics have emerged. The polymer is observed to mildly reorient with respect to the highly ordered air interface under hydrophobic liquids and at hydrophobic surfaces. In contrast to the weak influence of the hydrophobic interfaces, significant reorganization is observed at hydrophilic interfaces.

Acknowledgment. We thank Dr. Steven J. Choquette for his assistance in the acquisition of the Raman spectra and Denis Lehane and Dr. Robert Bohn in performing the DFT calculations. Dr. Yang and Dr. Wilson were NIST National Research Council postdoctoral research associates.

Supporting Information Available: Complete calculations of the dPS thickness dependence of the interface Frensel factors for the air/polymer, hexane/polymer, and water/polymer; spectra of the air/polymer interface before and after UV-ozone treatment; and simulated VR-SFG spectra based on DFT calculated hyperpolarizabilities. This material is available free of charge via the Internet at http://pubs.acs.org.

References and Notes

(1) Buck, M.; Himmelhaus, M. *J. Vac. Sci. Technol. A* **2001**, *19*, 2712−2736.
(2) Richmond, G. L. *Annu. Rev. Phys. Chem.* **2001**, *52*, 357−389.
(3) Miranda, P. B.; Shen, Y. R. *J. Phys. Chem. B* **1999**, *103*, 3292−3307.
(4) Bain, C. D. *J. Chem. Soc., Faraday Trans.* **1995**, *91*, 1281−1296.
(5) Shen, Y. R. *Nature (London)* **1989**, *337*, 519−525.
(6) Chen, Z.; Shen, Y. R.; Somorjai, G. A. *Annu. Rev. Phys. Chem.* **2002**, *53*, 437−465.
(7) Zhang, D.; Dougal, S. M.; Yeganeh, M. S. *Langmuir* **2000**, *16*, 4528−4532.
(8) Briggman, K. A.; Stephenson, J. C.; Wallace, W. E.; Richter, L. J. *J. Phys. Chem. B* **2001**, *105*, 2785−2791.
(9) Oh-e, M.; Hong, S.-C.; Shen, Y. R. *Appl. Phys. Lett.* **2002**, *80*, 784−786.
(10) Schwab, A. D.; Dhinojwala, A. *Phys. Rev. E* **2003**, *67*, 021802-1-10.
(11) Gautam, K. S.; Schwab, A. D.; Dhinojwala, A.; Zhang, D.; Dougal, S. M.; Yeganeh, M. S. *Phys. Rev. Lett.* **2000**, *85*, 3854−3857.
(12) Wilson, P. T.; Briggman, K. A.; Wallace, W. E.; Stephenson, J. C.; Richter, L. J. *Appl. Phys. Lett.* **2002**, *80*, 3084−3086.
(13) Wilson, P. T.; Richter, L. J.; Wallace, W. E.; Briggman, K. A.; Stephenson, J. C. *Chem. Phys. Lett.* **2002**, *363*, 161−168.
(14) Richter, L. J.; Petralli-Mallow, T. P.; Stephenson, J. C. *Opt. Lett.* **1998**, *23*, 1594−1596.
(15) We identify certain commercial equipment, instruments, or materials in this article to specify adequately the experimental procedure. In no case does such identification imply recommendation or endorsement by the National Institute of Standards and Technology, nor does it imply that the materials or equipment identified are necessarily the best available for the purpose.
(16) http://www.bioptechs.com/Products/FCS2/fcs2.html.
(17) Zhuang, X.; Miranda, P. B.; Kim, D.; Shen, Y. R. *Phys. Rev. B* **1999**, *59*, 12632−12640.
(18) Varsanyi, G. *Vibrational Spectra of Benzene Derivatives*; Academic Press: New York, 1969.
(19) Density functional theory calculations were performed with the B3-LYP hybrid functional and a 6-31/G** basis set with the Gaussian 98 program.[15,20]
(20) Gaussian 98, Revision A.9: Frisch, M. J.; Trucks, G. W.; Schlegel, H. B.; Scuseria, G. E.; Robb, M. A.; Cheeseman, J. R.; Zakrzewski, V. G.; Montgomery Jr, J. A.; Stratmann, R. E.; Burant, J. C.; Dapprich, S.; Millam, J. M.; Daniels, A. D.; Kudin, K. N. O.; Strain, F. M. C.; Farkas, O.; Tomasi, J.; Barone, V.; Cossi, M.; Cammi, R.; Mennucci, B.; Pomelli, C.; Adamo, C.; Clifford, S.; Ochterski, J.; Petersson, G. A.; Ayala, P. Y.; Cui, Q.; Morokuma, K.; Malick, D. K.; Rabuck, A. D.; Raghavachari, K.; Foresman, J. B.; Cioslowski, J.; Ortiz, J. V.; Baboul, A. G.; Stefanov, B. B.; Liu, G.; Liashenko, A.; Piskorz, P.; Komaromi, I.; Gomperts, R.; Martin, R. L.; Fox, D. J.; Keith, T.; Al-Laham, M. A.; Peng, C. Y.; Nanayakkara, A.; Challacombe, M.; Gill, P. M. W.; Johnson, B.; Chen, W.; Wong, M. W.; Andres, J. L.; Gonzalez, C.; Head-Gordon, M.; Replogle, E. S.; Pople, J. A.; Gaussian Inc., Pittsburgh, PA, 1998.
(21) Wu, S. *Polymer Interface and Adhesion*; Marcel Deker: New York, 1982.
(22) Elliott, J. T.; Burden, D. L.; Woodward, J. T.; Sehgal, A.; Douglas, J. F. *Langmuir* **2003**, *19*, 2275−2283.
(23) Hirose, C.; Yamamoto, H.; Akamatsu, N.; Domen, K. *J. Phys. Chem.* **1993**, *97*, 10064−10069.
(24) Zhang, D.; Gutow, J.; Eisenthal, K. B. *J. Phys. Chem.* **1994**, *98*, 13729−13734.
(25) Ward, R. N.; Duffy, D. C.; Bell, G. R.; Bain, C. D. *Mol. Phys.* **1996**, *88*, 269−280.
(26) The index of refraction for Au in the IR is taken from: Palik, E. D., Ed.; *Handbook of Optical Constants of Solids*; Academic Press: Orlando, FL, 1985.
(27) Pliva, J.; Pin, A. S. *J. Mol. Spectrosc.* **1987**, *126*, 82−98.
(28) Langumir, I. *Science* **1938**, *87*, 493−500.
(29) Chen, Z.; Ward, R.; Tian, Y.; Eppler, A. S.; Shen, Y.-R.; Somorjai, G. A. *J. Phys. Chem. B* **1999**, *103*, 2935−2942.
(30) Liu, Y.; Messmer, M. C. *J. Phys. Chem. B* **2003**, *107*, 9774−9779.
(31) Wang, J.; Woodcock, S. E.; Buck, S. M.; Chen, C. Y.; Chen, Z. *J. Am. Chem. Soc.* **2001**, *123*, 9470−9471.
(32) Wang, J.; Paszti, Z.; Even, M. A.; Chen, Z. *J. Am. Chem. Soc.* **2002**, *124*, 7016−7023.
(33) Wang, J.; Buck, S. M.; Chen, Z. *J. Phys. Chem. B* **2002**, *106*, 11666−11672.
(34) Wang, J.; Buck, S. M.; Even, M. A.; Chen, Z. *J. Am. Chem. Soc.* **2002**, *124*, 13302−13305.
(35) Opdahl, A.; Somorjai, G. A. *Langmuir* **2002**, *18*, 9409−9412.
(36) Stanners, C. D.; Du, Q.; Chin, R. P.; Cremer, P.; Somorjai, G. A.; Shen, Y.-R. *Chem. Phys. Lett.* **1995**, *232*, 407−413.

MA049692S